American Mineralogist, Volume 62, pages 540–546, 1977

Structural transformations in natural ZnS

MICHAEL E. FLEET

Department of Geology, University of Western Ontario
London, Ontario, Canada

Abstract

Consideration of possible transformation mechanisms in natural ZnS suggests that ideal $2H$ wurtzite may transform toward a sphalerite structural state through isolated edge dislocations in individual hexagonal close-packed layers. Complete transformation to ideal $3C$ sphalerite appears to involve two distinct steps, a continuous transformation to an intermediate disordered layer sequence followed by a final discontinuous transformation; the latter is possibly only realised through recrystallisation. The $2H \rightarrow 3C$ structural transformation is illustrated by study of a sphalerite from Thomaston Dam, Connecticut, which yields X-ray diffraction patterns with broadened and diffuse reflections along reciprocal lattice rows with $h - k \neq 3n$ (equivalent hexagonal indices). This diffraction effect may be regarded as diagnostic of sphalerite (or sphalerite-like ZnS) which has formed by inversion of a more wurtzitic precursor.

In contrast, solid-state transformation in ideal $3C$ sphalerite is limited to the formation of deformation twins ([111] twin axis). This is illustrated by X-ray diffraction study of a deformed sphalerite from Austinville, Virginia.

Introduction

The crystal structure of sphalerite, the common mineral form of ZnS, is closely related to that of the polymorph wurtzite, and, in fact, it is this close structural relationship which is responsible for the crystallographic complexities of ZnS phases. The wurtzite structure consists of hexagonal close-packed arrays of Zn and S atoms separated by a translation of about 0.375 along the c axis. The structure may be represented by the $2H$ stacking sequence $ABABAB\ldots$ along the c axis, where A, B, and C (below) each represent a separate close-packed stacking unit of Zn–S dipoles (Fig. 1a). In contrast, the sphalerite structure is cubic close-packed and may be represented by the $3C$ stacking sequence $ABCABCAB\ldots$ along [111] directions (Fig. 1d). An infinite variety of stacking sequences between that of the ideal $2H$ and $3C$ end-member structures is possible. More than 150 ordered ZnS phases (polytypes) have been reported (Steinberger *et al.*, 1973), the majority of them in synthetic ZnS. Some degree of stacking disorder is very common, and completely disordered structures have also been reported (for example, Fleet, 1975, 1976).

Ideal $3C$ sphalerite is, of course, optically isotropic, but all other ZnS phases whose stacking sequences are crystallographically coherent are anisotropic; birefringence being proportional to the number of layers in hexagonal close-packing. This relationship will be discussed in a separate publication. In the present paper, the X-ray diffraction patterns of two anisotropic sphalerites, from Thomaston Dam, Connecticut and Austinville, Virginia, are interpreted by consideration of possible solid-state transformation mechanisms in ZnS. It is suggested that deformation of an ideal $3C$ sphalerite may only produce a twinned $3C$ structure and that sphalerite which has evidence of stacking disorder most probably represents partially transformed wurtzite (or non-cubic ZnS).

Thomaston Dam sphalerite

The Thomaston Dam, Connecticut, sphalerite occurs as aggregates of dark brown grains in quartz veinlets within schistose country rocks. The present observations were made on a hand specimen from the Dana Mineral Collection of the University of Western Ontario (No. 2519). A second hand specimen was obtained from Ward's Natural Science Establishment, Rochester, New York. Both mineral specimens were labelled 'wurtzite' which is consistent with

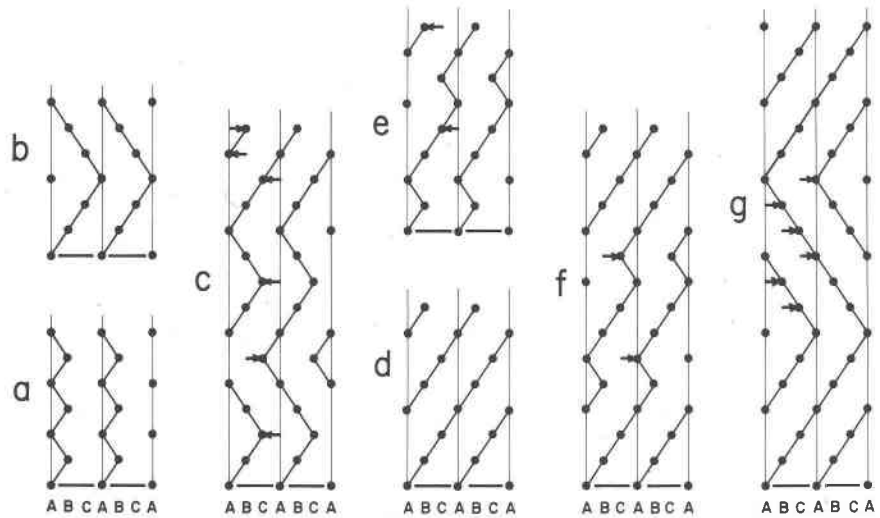

Fig. 1. Representation of (11.0) layer projections two unit-cells wide of various ZnS stacking sequences: (a) 2*H* wurtzite; (b) 6*H* wurtzite; (c) disordered sphalerite produced from 2*H* wurtzite by isolated edge dislocations; (d) 3*C* sphalerite; (e) disordered sequence produced from 2*H* wurtzite by deformation block faults; (f) disordered sphalerite produced from 3*C* sphalerite by deformation block faults; (g) twin lamella in 3*C* sphalerite formed by deformation faults. Dots represent individual Zn–S dipoles; heavy lines emphasize nearest-neighbor relations; *A*, *B*, *C* indicate close-packed stacking positions; arrows indicate partial dislocations; hexagonal *c* axis, cubic [111] vertical.

the appearance of the ZnS in hand specimen. Many of the grains have a platy, tabular or columnar hexagonal habit and have abundant parallel growth features with hexagonal symmetry.

Small crystal fragments (less than 1.0 mm in longest dimension) of this sphalerite are anisotropic and tend to be optically homogeneous. Lamellar bands of higher birefringence and wider isotropic bands are occasionally present in the larger fragments. The crystal (0.04 × 0.05 × 0.1 mm) used for the precession photograph (Fig. 2) has a birefringence of 0.0033.

Precession photographs of the Thomaston Dam sphalerite (Fig. 2) show reflections characteristic of twinned sphalerite ([111] twin axis), with prominent diffraction streaks along reciprocal lattice rows with $h - k \neq 3n$ (equivalent hexagonal indices). Each crystal is twinned about only *one* of the four symmetry equivalent [111] directions. This [111] direction corresponds to the c^* axis of the wurtzite from which, it is argued below, the sphalerite developed. The complete orientation relationship is [111]* sph | | c^* axis wtz, [$\bar{1}\bar{1}$2]* sph | | a^* axis wtz, [$\bar{1}$10] sph | | a axis wtz (Fig. 3). Twin-equivalent reflections have the same intensity, suggesting that the two twin orientations are equally represented.

The diffraction streaks are consistent with the presence of random stacking faults in close-packed layers (Wilson, 1949). In the model of Jagodzinski (1949) for growth faults in a close-packed sequence with $s = 3$, a fourth close-packed layer continues a 2*H* hexagonal arrangement with probability $1 - \alpha$ and continues a 3*C* cubic arrangement with probability β. Following Singer and Gashurov (1963), the diffraction intensity along a reciprocal lattice row with (h –

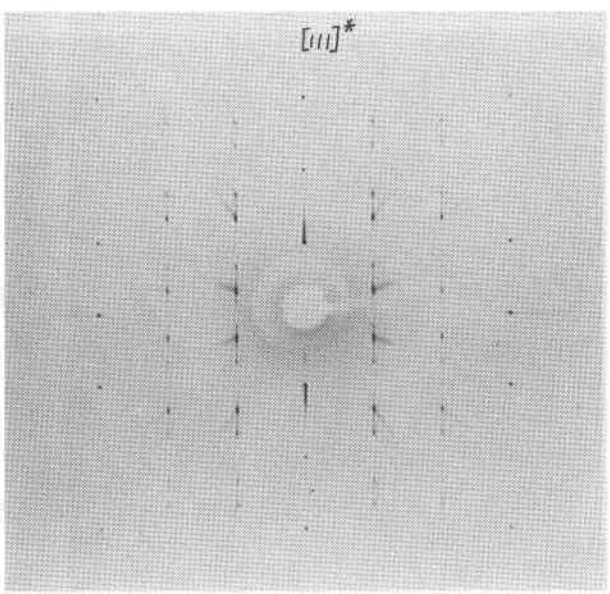

Fig. 2. Zero-layer, [$\bar{1}$10] axis precession photograph of Thomaston Dam sphalerite: Mo$K\alpha$ radiation, $\mu = 30°$, 3 days exposure: interpretation in Fig. 3.

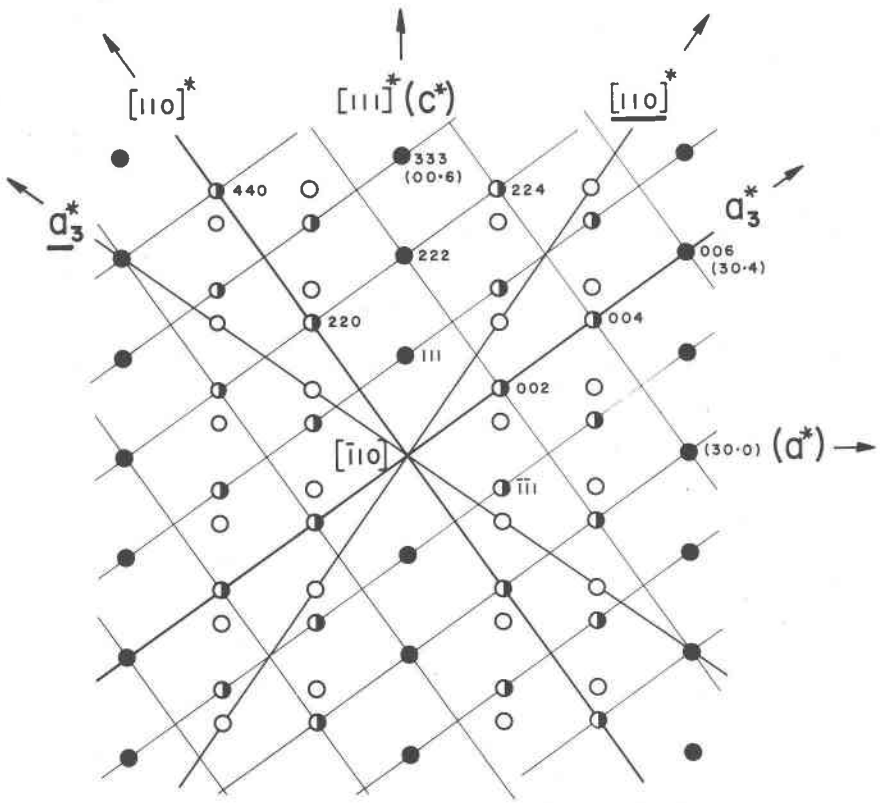

Fig. 3. Interpretation of precession photographs of Figs. 2 and 5, showing twinned 3C sphalerite lattices related by rotation about [111] and oriented relative to the close-packed direction in 2H wurtzite: circles closed on LHS, reflections of twin orientation 1; open circles, reflections of twin orientation 2; full circles, reflections common to twin orientations 1 and 2 and 2H wurtzite.

$k) \neq 3n$ is given by

$$I \simeq |F|^2 \sum_{\nu=2}^{5} \frac{K_\nu(1 - X_\nu^2)}{1 - 2X_\nu \cos A_3 + X_\nu^2}, \qquad (1)$$

where F is the layer structure factor (Müller, 1952); A_3 is the distance, in degrees, along the row, adjacent 2H hexagonal maxima being separated by π degrees; K_ν, X_ν are functions of α and β. This theory has been applied to the Thomaston Dam sphalerite following the procedure of Fleet (1976). The intensity distribution along a 10.l lattice row (equivalent hexagonal indices) from $A_3 = 0°$ (10.0 of 2H wurtzite) to $A_3 = 360°$ (10.2 of 2H wurtzite) is reproduced in Figure 4. There are no maxima at positions corresponding to 2H reflections, so that the values of X_2, X_3, K_2, and K_3 in equation (1) have to be zero. Moreover, the diffraction maxima are not asymmetrical nor displaced from ideal positions, and they do not have lateral plateaus, and thus $\alpha = \beta$. The best fit of the calculated distribution was obtained for $\alpha = 0.825$, so that the fraction of hexagonal close-packed ZnS layers is about 0.18. The small diffraction maxima at $A_3 = 60°$ and 300° appear to be equivalent to 10.1 and 10.5 of 6H wurtzite. However, the agreement between observed and calculated intensities is not too satisfactory (Fig. 4), and it might be concluded that the twinned sphalerite contains admixed disordered 6H wurtzite. It will be argued below that the presence of these maxima is consistent with the mode of formation and crystallographic state of the Thomaston Dam sphalerite, but it should be appreciated that the intensity associated with them has been ignored in determining α, and to this extent the value quoted is an approximate one.

Austinville sphalerite

This sample was from a banded sphalerite galena ore from Austinville, Virginia, collected by Dr. J. R. Craig. Narrow anisotropic twin lamellae within a weakly anisotropic matrix are visible in thin sections polished on both sides. The twin lamellae are frequently curved, somewhat lensoid, and sometimes intersect a second set of lamellae. Serrated grain boundaries, with the serrations coincident with twin lamellae, and offsets at the intersections of twin lamellae have been observed, indicative of relative

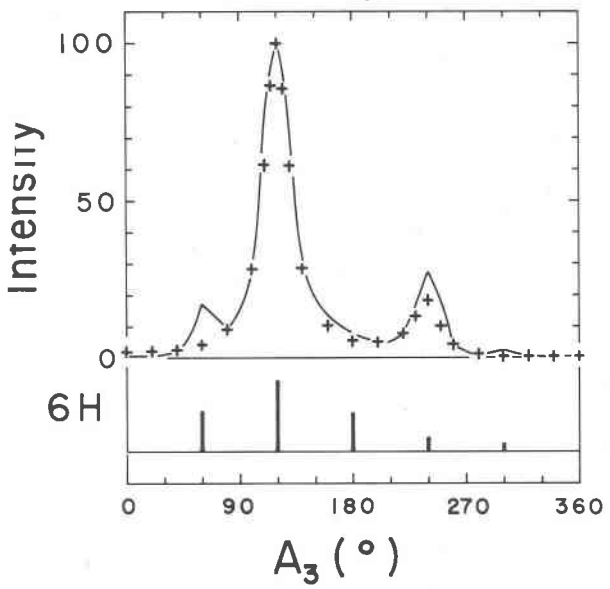

Fig. 4. Calculated and observed intensity distribution for 10.*l* reciprocal lattice row (equivalent hexagonal indices) of Thomaston Dam sphalerite recorded on precession film with Mo$K\alpha$ radiation, μ = 30°. Calculated distributions (plus signs) are according to Jagodzinski (1949) with α = 0.825. Observed distributions are averages of 10.*l* and 10.$\bar{l}$ data scaled with I_{max} = 100: vertical bars indicate calculated intensity of 6*H* wurtzite; A_3 = 0, 180 and 360° correspond, respectively, to positions of 10.0, 10.1, and 10.2 of ordered 2*H* wurtzite.

block movement within grains on either side of the twin lamellae. The appearance of the lamellae is strongly suggestive of deformation twins, and this is consistent with the structural setting of the ore body. A few sphalerite areas are wholly recrystallised to fine-grained massive twinned sphalerite with well-developed shear structures preserved.

Precession photographs indicate a twinned sphalerite diffraction pattern (Fig. 5). Although the reflections of both host and twin lamellae are radially diffuse, due to mosaic spread of the crystallites within the crystals examined, there is no evidence of reflection broadening along lattice rows with $h - k \neq 3n$ (equivalent hexagonal indices). Also, the fault sensitive reflections are not displaced from their ideal positions. Hence, there is no indication of coherent stacking faults in this sphalerite. Deformation block faults are not present within the lamellar areas, and the sphalerite appears to have deformed wholly via a twinning process.

Solid state transformations in ZnS

There is little doubt that ZnS phases are susceptible to transformation by periodic slip processes. This is a reflection of their close-packed structures, which allow two equivalent positions for every layer of stacking units. In this regard they are analogous to close-packed metals. However, the largely covalent, tetrahedrally disposed Zn–S bonds place additional constraints on the type of slip processes which may occur in them. A slip plane must pass through the Zn-S bonds inclined to the hexagonal *c* axis (the type II plane of Kelley and Groves, 1970, Chap. 8). Clearly a non-unit translation on a type I slip plane would give a non-tetrahedral ZnS configuration in the vicinity of the slip plane. Also, the small vertical separation of the Zn and S atoms across the type II slip planes and the strong directional nature of the sp^3 tetrahedral bonds preclude a slip movement that would result in these atoms overriding one another.

Possible transformation mechanisms may be divided into three categories:

(1) isolated or coupled partial edge dislocations: an isolated edge dislocation transforms the 2*H* sequence *ABABABA* . . into *ABACABA* . . ;

(2) deformation block faults: the sequence *ABABABA* . . is transformed into *ABACBCB* . . ;

(3) spiral dislocation: transforms to a periodic block faulted sequence.

When movement takes place along a slip plane, the crystalline region within which it is operating is in an excited energy state. Thus the most likely mechanism for slip movement is the one which results in the

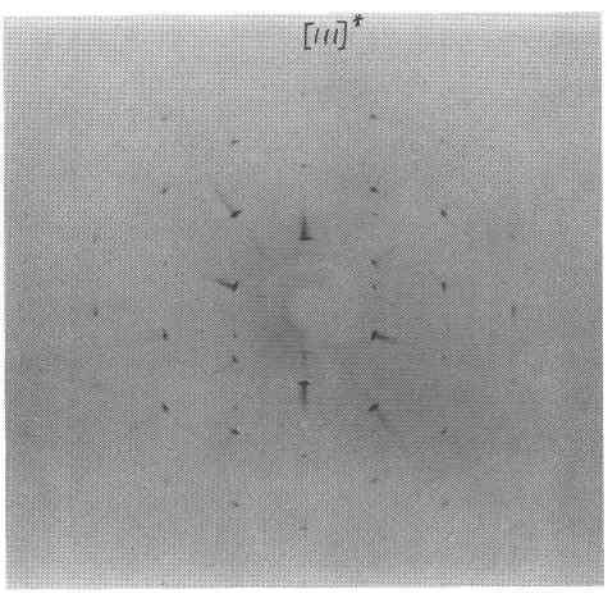

Fig. 5. Zero-layer, [$\bar{1}$10] axis precession photograph of Austinville sphalerite: Mo$K\alpha$ radiation, μ = 30°, 4 days exposure: interpretation in Fig. 3.

breaking of fewest bonds at any one instant. It is partly for this reason that the first category of transformation mechanism is thought to be the most likely one operating in natural hexagonal and rhombohedral ZnS. Consider the passage of a partial edge dislocation, isolated by two type II slip planes, through 2*H* wurtzite. Let it shift dipoles from the *B* position to the *C* position (Fig. 6a). Only two of the six Zn–S bonds per dipole need be broken and remade: the other four are merely rearranged during the movement process. The dislocation is initiated in the outermost layer of a coherent crystalline block, perhaps initially as a point, but it must develop into a line to pass through the block. The dislocation is very narrow and affects only nearest-neighbor atoms. Hence its associated energy is minimal. Random initiation of isolated edge dislocations would transform the 2*H* stacking sequence of Figure 1a into the stacking sequence of Figure 1c. If the crystal is transforming in a way which maximises the number of cubic close-packed layers, the structure becomes effectively 'locked-in' when the last repeated hexagonal close-packed layer is lost from the sequence. A minimum of layer movement is required to arrive at this condition. Complete solid-state conversion of 2*H* wurtzite to ideal (untwinned) 3*C* sphalerite requires considerable further rearrangement of the close-packed layers.

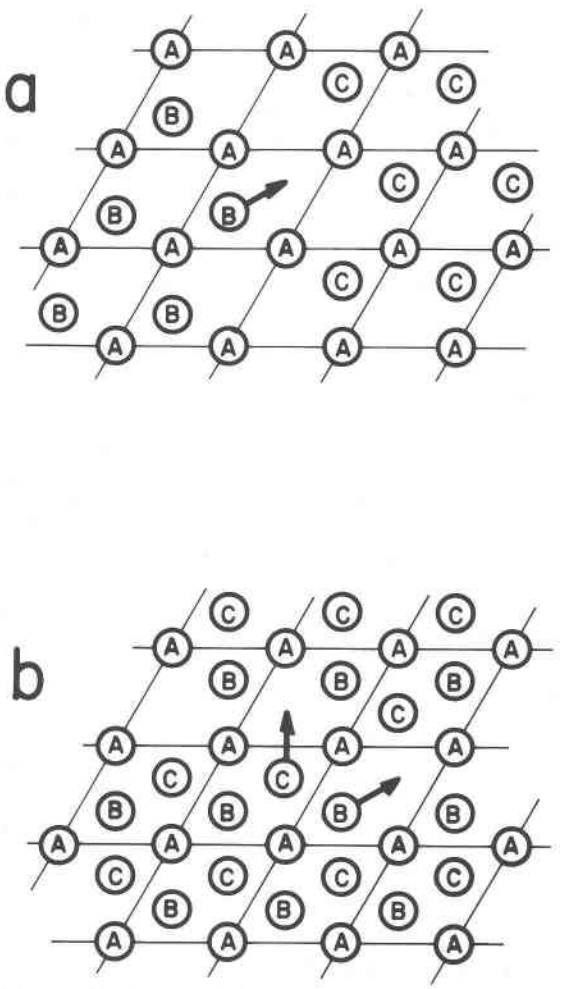

Fig. 6. (a) Movement of partial edge dislocation in 2*H* wurtzite, transferring stacking units within one layer from *B* position to *C* position; *c* axis projection. (b) Movement of coupled partial edge dislocation in 3*C* sphalerite transferring stacking units from *B* to *C* position within one layer and from *C* to *B* position within an adjacent layer; [111] projection; partial dislocations indicated by arrows.

Although only one slip plane is required in the block fault transformation, the dislocation zone must be several unit cells in width and must extend well into the stacking layers above the slip plane. Therefore, in wurtzite it is not favored relative to the isolated edge dislocation mechanism, and this argument is supported by the absence of asymmetrically broadened and displaced intensity maxima in disordered natural ZnS (Fleet, 1976, and present study), which are produced in block faulted structures (Paterson, 1952).

The energy associated with movement along a spiral dislocation must be relatively extremely high. Although this transformation mechanism has been invoked for synthetic wurtzite polytypes (Alexander *et al.*, 1970), there is no evidence that it had any role in the development of natural ZnS polytypes. In fact, there is a rather remarkable correlation between crystal habit and periodicity in many natural ZnS polytypes (for example, Evans and McKnight, 1959), which seems to confirm that they developed by crystal growth.

Isolated edge dislocations are not possible in the ideal 3*C* sphalerite structure, since stacking units would be translated directly above or below adjacent units; for example, *ABCABCAB* . . would be transformed to *ABCACCAB* . . , and so on. However, coupled edge dislocations (Fig. 6b), analogous to the extrinsic stacking fault of Kelley and Groves are possible, transforming *ABCABCAB* . . to *ABCACBAB* . . , and so on. The coupled edge dislocation is of higher energy than the isolated edge dislocation, which suggests that 3*C* sphalerite should be less susceptible to solid-state transformation than 2*H* wurtzite. Also, although this mechanism would allow the fairly direct transformation to a twinned 3*C* structure, transformation to the ideal 2*H* structure would

require several phases of dislocation events and does not appear to be a very favored process.

The absence of asymmetrically broadened and displaced reflections in the Austinville sphalerite suggests that deformation block faulting as illustrated in Figure 1f is not present. However, closely-spaced deformation faults as illustrated in Figure 1g would result in the formation of 3*C* twin lamellae with a considerable net displacement of the enclosing 3*C* matrix blocks, the transformation requiring a considerable excess of energy, resulting in local disruption and straining of the structure.

Discussion

The structural state of the Thomaston Dam sphalerite is clearly that of a disordered stacking sequence similar to the one depicted in Figure 1c with a fraction of hexagonal close-packed layers (W_h) of about 0.18 and a large number of 6*H* stacking units. Whilst the X-ray diffraction pattern clearly rules out solid-state transformation by deformation block faulting as a possible origin for this sphalerite, it cannot differentiate between direct crystal growth and transformation by isolated edge dislocations. On the other hand, the hand specimen apparently shows that the sphalerite is pseudomorphing earlier wurtzite, so that it can be stated with some confidence that the Thomaston Dam sphalerite is a solid-state transformation product of a more wurtzitic precursor. Assuming this to be 2*H* wurtzite, the Thomaston Dam sphalerite indicates the $2H \rightarrow 3C$ solid-state phase transformation proceeds in at least two distinct steps: a rapid transformation to $W_h = 0.18$ and a sporadic, rate-controlling transformation from $W_h = 0.18$ to ideal 3*C* sphalerite. This, of course, is entirely consistent with the transformation mechanism as discussed in the previous section. Also the 3*C* sphalerite bands in the Thomaston Dam sphalerite have a distinctly darker colour than the disordered matrix and may, in fact, be primary in nature. Certainly one suspects that complete solid-state transformation to ideal 3*C* sphalerite is not a very practical proposition, and the final step may be realized in nature only through a first-order (recrystallisation) phase change. This is supported by studies on a sample of Pribram, Czechoslovakia, wurtzite, which shows a solid-state transformation to $W_h = 0.63$ (Fleet, 1976) followed by first-order transformation to 3*C* sphalerite, the latter indicated by raggedly terminated isotropic bands and lamellae in disordered wurtzite. Clearly details of the $2H \rightarrow 3C$ transformation must vary with mineral chemistry and physicochemical conditions.

Although twin lamellae within a 3*C* matrix could be produced by a coupled edge dislocation mechanism, the evidence in favor of closely-spaced deformation faults (Fig. 1g) as the origin of the twin lamellae in the Austinville sphalerite is quite compelling. The twin lamellae represent 'shear zones' within the individual sphalerite grains. Once movement is initiated along a single slip plane, the consequent disruption to the crystal structure along the dislocation front makes the slip plane a zone of weakness favoring corresponding slip movements on neighboring planes. When the stacking units have moved to the positions of the inverted 3*C* structure, the structure becomes locked, and additional shear stress is relieved by slip planes higher up in the layer sequence. Such a transformation process would result in much local disruption of the sphalerite structure, and presumably the incoherent nature of the twin lamellae within the 3*C* matrix is a reflection of this.

In light of the present observations it is predicted that solid-state transformation in sphalerite is limited to the formation of deformation twins, which are commonly observed (Ramdohr, 1969). The ideal 3*C* structure is effectively locked against isolated edge dislocations. The external energy input required to initiate slip plane movement is relatively large, and when this condition is realised the structure will deform by twin formation in preference to block faulting. Solid-state transformation of 3*C* sphalerite to wurtzite is not expected to be a very probable process, and I am not aware of a documented example of it occurring in nature. On the other hand, the 2*H* wurtzite structure appears to allow a partial solid-state transformation to sphalerite, and in agreement with this natural wurtzite appears unstable relative to sphalerite under postformation conditions. Thus, the structural relations between wurtzite and sphalerite allow only for a 'one-way' solid-state transformation (*cf.* Baars and Brandt, 1973), and this must be a complicating factor in assessing the thermodynamic stability of ZnS phases.

Finally, it appears from this study that in sphalerite (and sphalerite-like ZnS) the presence of broadened and diffuse X-ray reflections along lattice rows with $h - k \neq 3n$ (equivalent hexagonal indices) must indicate transformation from a more wurtzitic precursor.

Acknowledgments

Thanks go to Professor G. G. Suffel, Western Ontario, and Dr. J. R. Craig, Virginia Polytechnic Institute and State University, for providing samples. The study was supported by a National Research Council of Canada operating grant.

References

Alexander, E., Z. H. Kalman, S. Mardix and I. T. Steinberger (1970) The mechanism of polytype formation in vapor-phase grown ZnS crystals. *Phil. Mag., 21,* 1237–1246.

Baars, J. and G. Brandt (1973) Structural phase transitions in ZnS. *J. Phys. Chem. Solids, 34,* 905–909.

Evans, H. T., Jr. and E. T. McKnight (1959) New wurtzite polytypes from Joplin, Missouri. *Am. Mineral., 44,* 1210–1218.

Fleet, M. E. (1975) Wurtzite: long-period polytypes in disordered 2*H* crystals. *Science, 190,* 885–886.

——— (1976) Stacking disorder in natural 2*H* wurtzite. *J. Appl. Crystallogr., 9,* 190–192.

Jagodzinski, H. (1949) Eindimensionale Fehlordnung in Kristallen und ihr Einfluss auf die Röntgeninterferenzen. II. Berechnung der fehlgeordneten dichtesten Kugelpackungen mit Wechselwirkungen der Reichweite 3. *Acta Crystallogr., 2,* 208–214.

Kelly, A. and G. W. Groves (1970) *Crystallography and Crystal Defects.* Longman, London.

Müller, H. (1952) Die eindimensionale Umwandlung Zinkblende-Wurtzit und die dabei auftretenden Anomalien. *Neues Jahrb. Mineral. Abh., 84,* 43–76.

Paterson, M. S. (1952) X-ray diffraction by face-centred cubic crystals with deformation faults. *J. Appl. Phys., 23,* 805–811.

Ramdohr, P. (1969) *The Ore Minerals and their Intergrowths.* Pergamon, Oxford.

Singer, J. and G. Gashurov (1963) Faulting in ZnS: Analysis by a two-parameter model. *Acta Crystallogr., 16,* 601–604.

Steinberger, I. T., I. Kiflawi, Z. H. Kalman and S. Mardix (1973) The stacking faults and partial dislocations in structure transformations of ZnS crystals. *Phil. Mag., 27,* 159–175.

Wilson, A. J. C. (1949) *X-ray Optics,* first ed. Methuen, London.

Manuscript received, October 12, 1976; accepted for publication, January 6, 1977.